PERGAMON

Available at
www.ElsevierComputerScience.com
POWERED BY SCIENCE DIRECT®

Pattern Recognition 37 (2004) 1987–1998

PATTERN RECOGNITION
THE JOURNAL OF THE PATTERN RECOGNITION SOCIETY

www.elsevier.com/locate/patcog

Palmprint classification using principal lines

Xiangqian Wu[a], David Zhang[b,*], Kuanquan Wang[a], Bo Huang[a]

[a] *School of Computer Science and Technology, Harbin Institute of Technology (HIT), Harbin 150001, China*
[b] *Department of Computing, Biometric Research Centre, Hong Kong Polytechnic University, Hung Hum, Kowloon, Hong Kong*

Received 30 January 2004; accepted 12 February 2004

Abstract

This paper proposes a novel algorithm for the automatic classification of low-resolution palmprints. First the principal lines of the palm are defined using their position and thickness. Then a set of directional line detectors is devised. After that we use these directional line detectors to extract the principal lines in terms of their characteristics and their definitions in two steps: the potential beginnings ("line initials") of the principal lines are extracted and then, based on these line initials, a recursive process is applied to extract the principal lines in their entirety. Finally palmprints are classified into six categories according to the number of the principal lines and the number of their intersections. The proportions of these six categories (1–6) in our database containing 13,800 samples are 0.36%, 1.23%, 2.83%, 11.81%, 78.12% and 5.65%, respectively. The proposed algorithm has been shown to classify palmprints with an accuracy of 96.03%.

Keywords: Biometrics; Palmprint classification; Principal lines; Life line; Head line; Heart line

1. Introduction

Computer-aided personal recognition is becoming increasingly important in our information society, and in this field biometrics is one of the most important and reliable methods [1,2]. The most widely used biometric feature is the fingerprint [3,4] and the most reliable feature is the iris [1,5,6]. However, it is very difficult to extract small unique features (known as minutiae) from unclear fingerprints [3,4] and iris input devices are very expensive. Yet other biometric features, such as the face [7,8] and voice [9,10], are less accurate. A palm is the inner-surface of the hand between the wrist and the fingers [1]. A palmprint is defined as the prints on a palm, which are mainly composed of the palm lines and ridges. A palmprint, as a relatively new biometric feature, has several advantages compared with other currently available features [11]: palmprints contain more information than fingerprints, so they are more distinctive; palmprint capture devices are much cheaper than iris devices; palmprints contain additional distinctive features such as principal lines and wrinkles, which can be extracted from low-resolution images; and last, by combining all of the features of a palm, such as palm geometry, ridge and valley features, and principal lines and wrinkles, it is possible to build a highly accurate biometrics system. Given these advantages, in recent years, palmprints have been investigated extensively in automated personal authentication. Duta et al. [12] extracted some points (called "feature points") on palm-lines from offline palmprint images for verification. Zhang et al. [13] used 2-D Gabor filters to extract the texture features from low-resolution palmprint images and employed these features to implement a highly accurate online palmprint recognition system. Han et al. [14] used Sobel and morphological operations to extract line-like features from palmprints. Kumar et al. [15] integrated line-like features and hand geometric features for personal verification.

All of these palmprint authentication methods require that the input palmprint should be matched against a large number of palmprints in a database, which is very time

* Corresponding author. Tel.: +852-2766-7271; fax: +852-2774-0842.
E-mail address: csdzhang@comp.polyu.edu.hk (D. Zhang).

0031-3203/$30.00 © 2004 Pattern Recognition Society. Published by Elsevier Ltd. All rights reserved.
doi:10.1016/j.patcog.2004.02.015

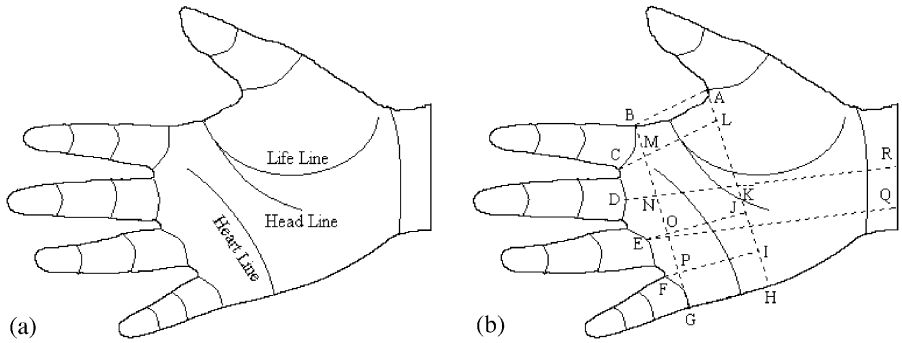

Fig. 1. (a) The typical principal lines on a palm; (b) Defined points and lines on a palm.

consuming. To reduce the search time and computational complexity, it is desirable to classify palmprints into several categories such that the input palmprint need be matched only with the palmprints in its corresponding category, which is a subset of palmprints in the database. Like fingerprint classification [16,17], palmprint classification is a coarse-level matching of palmprint. Shu et al. [18] used the orientation property of the ridges on palms to classify offline high-resolution palmprints into six categories. Obviously, this classification method is unsuitable for low-resolution palmprints because it is impossible to obtain the orientation of the ridges from low-resolution images. As the first attempt at online low-resolution palmprint classification, we classify palmprints by taking into account their most visible and stable features, i.e. the principal lines. Most palmprints show three principal lines: heart line, head line and life line (Fig. 1(a)). In this paper, we describe how these principal lines may be extracted according to their characteristics, which allows us then to classify palmprints into six categories by the number of principal lines and the number of their intersections.

The rest of this paper is organized as follows. Section 2 presents some definitions and notation. Section 3 develops a key point detection technique. Section 4 details how principal lines are extracted. Section 5 explains the criteria for palmprint classification. Section 6 reports some experimental results, and Section 7 provides some conclusions.

2. Definitions and notations

Because there are many lines in palmprints, it is very difficult—without explicit definitions—to distinguish principal lines from mere wrinkles. When people discriminate between principal lines and wrinkles, the position and thickness of the lines play a key role. Likewise, we define the principal lines according to their positions and thickness.

To determine the positions of principal lines, we first define some points and straight lines in a palmprint. Fig. 1(b) illustrates these points and straight lines. Points A, B, C, F and G are the root points of the thumb, forefinger and little finger. Points D and E are the midpoints of the root line of the middle finger and the ring finger. Line BG is the line passing through Points B and G. Line AH is the straight line parallel with Line BG, intersecting with the palm boundary at Point H. Line AB is the line passing through Points A and B. Line CL is the straight line parallel with Line AB and intersecting with Lines BG and AH at Points M and L, respectively. Line GH passes through Points G and H. Lines FI and EJ are the straight lines parallel with Line GH and intersecting with Lines BG and AH at Points P, I, J and O, respectively. K is the midpoint of straight line segment AH. Line DR passes through Points D and K. Line EQ is the straight line parallel with Line DR and intersects with the palm boundary at Point Q. Using these points and lines, we define the principal lines as below:

The ***heart line*** is a smooth curve that satisfies the following conditions (Fig. 2(a)):

(1) Originating from region GHIP;
(2) Running across line-segment OJ;
(3) Not running across line-segment AH.

The ***head line*** is a smooth curve that satisfies the following conditions (Fig. 2(b)):

(1) It is not the same curve as the extracted heart line;
(2) Originating from region ABML;
(3) Running across straight-line DR;
(4) The straight line which passes the two endpoints of this curve runs across line-segment EQ;
(5) The straight line which passes the two endpoints of this curve does not run across line-segment BG.

The ***life line*** is a smooth curve that satisfies the following conditions (Fig. 2(c)):

(1) Originating from region ABML;
(2) Running across line-segment AH;
(3) The straight line which passes the two endpoints of this curve does not run across line-segment EQ.

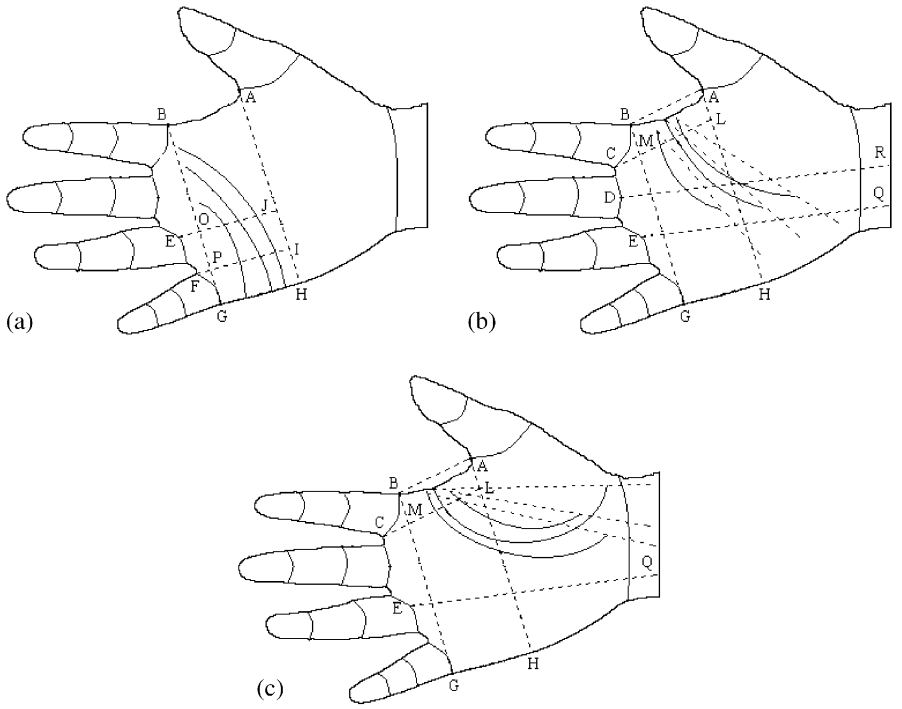

Fig. 2. Definitions of principal lines: (a) the heart line, (b) the head line and (c) the life line.

In our work, we describe principal lines according to following three basic rules. First, the number of each type of principal line occurring in a palmprint is less than or equal to 1. If more than one line satisfies the same conditions, we keep the one with the greatest average magnitude. Second, we do not take into account broken principal lines. When a principal line is broken at some place, we regard the broken point as its endpoint. Third, we regard each principal line as a curve without branches. Thus, if there are branches, we keep the smoothest curve and discard the others.

3. Key points detection

Given the above definitions, we must first detect a set of points and lines before we can extract principal lines. Point A, B, C, D, E, F and G are the key points from which the other points and the defined lines can be easily obtained using their definitions (Fig. 1(b)). All images used in this paper were captured online using a CCD-camera-based device fitted with three pegs. One peg separates the first and middle fingers, another the middle and third fingers, and the final peg separates the third finger and little finger. These pegs are broad enough to stretch the fingers apart, thereby allowing us to detect the key points.

Detecting key points begins with extraction of the boundary of the palm by first smoothing the original image (Fig. 3(a)) using a low-pass filter and a threshold to convert it into a binary image (Fig. 3(b)) and then tracing the boundary of the palm (Fig. 3(c)). In our database, a small portion of some palm images below the little finger is not captured. In these cases, we use the corresponding boundary segment of the image to represent the missing palm boundary segment.

Detecting point A (Fig. 3(d)):

(1) Find a point (X) on the thumb boundary;
(2) Find the point (Y) on the palm boundary whose column index is less l than that of point X (here, $l = 30$);
(3) In all points on the palm boundary segment between point X and point Y, find the point which is farthest from line XY as point A.

Detecting points C, D, E and F:

(1) Use straight lines, L_1, L_2, L_3, L_4, L_5 and L_6, to fit the segments of the boundary of the forefinger, middle finger, third finger and little finger (Fig. 3(d)):

$$L_i: y = k_i x + b_i, \tag{1}$$

$$k_i = \frac{\sum_{k=1}^{M_i} x_i^k \times \sum_{k=1}^{M_i} y_i^k - M_i \times \sum_{k=1}^{M_i} (x_i^k \times y_i^k)}{\left(\sum_{k=1}^{M_i} x_i^k\right)^2 - M_i \times \sum_{k=1}^{M_i} (x_i^k)^2}, \tag{2}$$

$$b_i = \frac{\sum_{k=1}^{M_i} y_i^k - k_i \times \sum_{k=1}^{M_i} x_i^k}{M_i}, \tag{3}$$

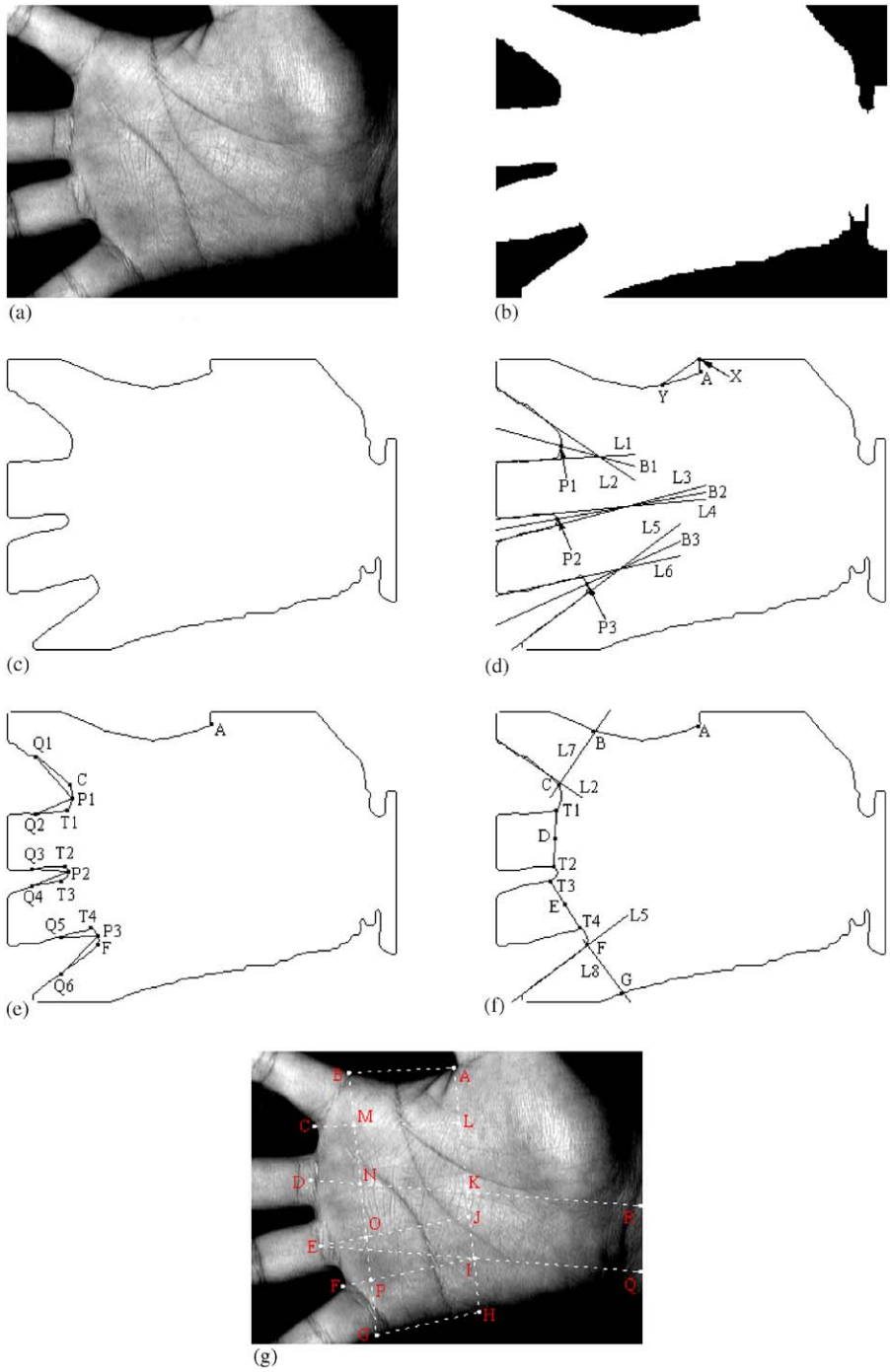

Fig. 3. The process of key point detection.

where $\{(x_i^k, y_i^k)\}_{k=1}^{M_i}$, $(i = 1, \ldots, 6)$ are the coordinates of the points on the segments of the boundary of the forefinger, middle finger, third finger and little finger, respectively; M_i is the total number of points on the corresponding segment.

(2) Compute the bisectors (B_1, B_2 and B_3) of the angles formed by L_1 and L_2, L_3 and L_4, and L_5 and L_6:

$$B_i\colon\ y = K_i x + B_i, \tag{4}$$

$$K_i = \frac{k_{2\times i-1} \times \sqrt{1+k_{2\times i}^2} + k_{2\times i} \times \sqrt{1+k_{2\times i-1}^2}}{\sqrt{1+k_{2\times i-1}^2} + \sqrt{1+k_{2\times i}^2}}, \tag{5}$$

$$B_i = \frac{b_{2\times i-1} \times \sqrt{1+k_{2\times i}^2} + b_{2\times i} \times \sqrt{1+k_{2\times i-1}^2}}{\sqrt{1+k_{2\times i-1}^2} + \sqrt{1+k_{2\times i}^2}}, \tag{6}$$

where $i = 1, 2, 3$; $k_1 \sim k_6, b_1 \sim b_6$ are computed by Eqs. (2)–(3). The intersections of B_1, B_2 and B_3 with palm boundary segments between the fingers are Point P_1, P_2 and P_3 (Fig. 3(d));

(3) Find the points Q_1 and Q_2 on the boundary of forefinger and middle finger, whose column index is less l_1 than that of point P_1 (here $l_1 = 30$), and link up P_1Q_1 and P_1Q_2 (Fig. 3(e));
(4) In all points on the finger boundary segment between point P_1 and point Q_1, find the point which is farthest from line P_1Q_1 as one root point of the forefinger, C (Fig. 3(e));
(5) In all points on the finger boundary segment between point P_1 and point Q_2, find the point which is farthest from line P_1Q_2 as one root point of the middle finger, T_1 (Fig. 3(e));
(6) The root points of the middle finger, ring finger and little finger, T_2, T_3, T_4 and F, are obtained using the same technique as described in Step 3–5 (Fig. 3(e));
(7) Link up T_1T_2 and T_3T_4, and take their midpoints as points D and E (Fig. 3(f));

Detecting Points B and G (Fig. 3(f)):

(1) Draw the perpendicular of line L_2 from point C, L_7, and intersect with palm boundary at point B;
(2) Draw the perpendicular of line L_5 from point G, L_8, and intersect with palm boundary at point G.

Fig. 3(g) shows the palmprint overlaid with the obtained key points and the defined lines.

4. Principal lines extraction

Palm-lines, including the principal lines and wrinkles, are a kind of roof edge. A roof edge is generally defined as a discontinuity in the first-order derivative of a gray-level profile [19]. In other words, the positions of roof edge points are the zero-cross points of their first-order derivatives. Moreover, the magnitude of the edge points' second-derivative can reflect the strength of these edge points [20]. We can use these properties to devise principal lines detectors. Given that the directions of principal lines are not constant, we should devise line detectors in different directions and then apply a suitable detector according to the local information of the principal lines.

4.1. Directional line detectors

Suppose that $I(x, y)$ denotes an image. We devise the horizontal line detector (the directional line detector in 0° direction). To improve the connection and smoothness of the lines, the image is smoothed along the line direction (horizontal direction) using a 1-D Gaussian function G_{σ_s} with variance σ_s:

$$I_s = I * G_{\sigma_s}, \tag{7}$$

where $*$ is the convolve operation.

The first- and the second-order derivatives in the vertical direction can be computed by convolving the smoothed image with the first- (G'_{σ_d}) and second- (G''_{σ_d}) order derivative of a 1-D Gaussian function G_{σ_d} with variance σ_d:

$$I' = I_s * (G'_{\sigma_d})^{\mathrm{T}} = (I * G_{\sigma_s}) * (G'_{\sigma_d})^{\mathrm{T}} = I * (G_{\sigma_s} * (G'_{\sigma_d})^{\mathrm{T}}) = I * H_1^0 \tag{8}$$

$$I'' = I_s * (G''_{\sigma_d})^{\mathrm{T}} = (I * G_{\sigma_s}) * (G''_{\sigma_d})^{\mathrm{T}} = I * (G_{\sigma_s} * (G''_{\sigma_d})^{\mathrm{T}}) = I * H_2^0, \tag{9}$$

where $H_1^0 = G_{\sigma_s} * (G'_{\sigma_d})^{\mathrm{T}}$, $H_2^0 = G_{\sigma_s} * (G''_{\sigma_d})^{\mathrm{T}}$; T is the transpose operation; $*$ is the convolve operation. H_1^0, H_2^0 are called the horizontal line detectors (*directional line detectors in* 0° *direction*).

The horizontal lines can be obtained by looking for the zero-cross points of I' in the vertical direction and their strengths are the values of the corresponding points in I'':

$$L_0^1(x, y) = \begin{cases} I''(x, y) & \text{if } I'(x, y) = 0 \text{ or} \\ & I'(x, y) \times I'(x+1, y) < 0, \\ 0 & \text{otherwise.} \end{cases} \tag{10}$$

Furthermore, we can determine the type of a roof edge (line), i.e. valley or peak, from the sign of the values in $L_0^1(x, y)$: plus signs represent valleys, while minus signs represent peaks. Since all palm-lines are valleys, the minus values in $L_0^1(x, y)$ should be discarded:

$$L_0^2(x, y) = \begin{cases} L_0^1(x, y) & \text{if } L_0^1(x, y) > 0, \\ 0 & \text{otherwise.} \end{cases} \tag{11}$$

Palm-lines are much thicker than ridges. For that reason, one or more thresholds can be used to remove ridges from L_0^2 and obtain a magnitude image L_0, which is called the directional line magnitude image in 0° direction.

The directional line detectors H_1^θ, H_2^θ in θ direction can be obtained by rotating H_1^0, H_2^0 with angle θ. The line points can be obtained by looking for the zero-cross points in $\theta + 90°$ direction. After discarding the peak roof edges and ridges, we can obtain the directional line magnitude image L_θ in θ direction.

There are two parameters σ_s and σ_d in these directional line detectors. σ_s controls the connection and smoothness of

the lines and σ_d controls the width of the lines which can be detected. Small σ_s results in poor connection and poor smoothness of the detected lines while large σ_s results in the loss of some short lines and of line segments whose curvatures are large. Thin roof edges cannot be extracted when σ_d is large, so we should choose the appropriate parameters ad hoc. In general, principal lines are long, narrow and somewhat straight, so for principal line extraction σ_s should be large while σ_d should be small. After tuning the values of σ_s and σ_d through a lot of experiments, we obtain the suitable ones for principal line extraction: $\sigma_s = 1.8$ and $\sigma_d = 0.5$. In this case,

$$H_1^0 = \begin{bmatrix} 0.0009 & 0.0027 & 0.0058 & 0.0092 & 0.0107 & 0.0092 & 0.0058 & 0.0027 & 0.0009 \\ 0.0065 & 0.0191 & 0.0412 & 0.0655 & 0.0764 & 0.0655 & 0.0412 & 0.0191 & 0.0065 \\ 0.0000 & 0.0000 & 0.0000 & 0.0000 & 0.0000 & 0.0000 & 0.0000 & 0.0000 & 0.0000 \\ -0.0065 & -0.0191 & -0.0412 & -0.0655 & -0.0764 & -0.0655 & -0.0412 & -0.0191 & -0.0065 \\ -0.0009 & -0.0027 & -0.0058 & -0.0092 & -0.0107 & -0.0092 & -0.0058 & -0.0027 & -0.0009 \end{bmatrix}, \quad (12)$$

$$H_2^0 = \begin{bmatrix} 0.0156 & 0.0211 & 0.0309 & 0.0416 & 0.0464 & 0.0416 & 0.0309 & 0.0211 & 0.0156 \\ 0.0257 & 0.0510 & 0.0954 & 0.1441 & 0.1660 & 0.1441 & 0.0954 & 0.0510 & 0.0257 \\ -0.0298 & -0.1125 & -0.2582 & -0.4178 & -0.4896 & -0.4178 & -0.2582 & -0.1125 & -0.0298 \\ 0.0257 & 0.0510 & 0.0954 & 0.1441 & 0.1660 & 0.1441 & 0.0954 & 0.0510 & 0.0257 \\ 0.0156 & 0.0211 & 0.0309 & 0.0416 & 0.0464 & 0.0416 & 0.0309 & 0.0211 & 0.0156 \end{bmatrix}. \quad (13)$$

The hysteretic threshold method [21], in which the high threshold is obtained automatically by using Otsu's method [22] to the non-zero points of L_θ^2 and the low threshold is chosen as the minimum value of the non-zero points of L_θ^2, is used for principal line extraction.

4.2. Extracting potential line initials of principal lines

The heart line is defined as a curve originating from Region GHIP (Fig. 2(a)) and the life line and head line are defined as the curves originating from Region ABML (Fig. 2(b) and (c)). Therefore we can extract the beginnings ("line initials") of the principal lines from these regions and then use these initials as the basis to extract the principal lines in their entirety. A careful examination of a palmprint reveals that each principal line will initially run almost perpendicular to its neighboring palm boundary segment—approximated here by line AB (life and head line) or line GH (heart line) (Fig. 3(g)). If we denote the slope angle of the corresponding line (line AB or line GH) as θ, then the directions of the line initials of the principal lines are close to $\theta + 90°$, so we first extract all lines in this region using the $\theta + 90°$ line detectors $H_1^{\theta+90°}$, $H_2^{\theta+90°}$. Each of these extracted line segments is a potential line initial of principal lines. Hence, we should extract lines from each of these line initials and then keep the principal lines according to their definitions. Fig. 4 shows these extracted lines: (a) is the original palmprint and (b) is the palmprint overlaid with the extracted potential line initials of the principal lines.

4.3. Extracting heart lines

Because principal lines do not curve greatly, it is a simple matter to use the current extracted part of the line to predict the position and direction of the next short part. Now, based on the extracted potential line initials, we devise a recursive process to extract the whole heart line.

Suppose that Curve *ab* in Fig. 5(a) is the extracted part of the heart line of the palmprint shown in Fig. 4(a). To extract the next part of the heart line, we trace back the extracted heart line *ab* from point *b* and get the *K*th point *c* (here $K = 20$). Since the heart line does not curve greatly, the region of interest (ROI), in which the next segment of heart line would be located, can be defined as a rectangular region $L \times W$ whose center point is point *b*. Point *c* is the midpoint of one border whose length is W. W is a predefined value (here $W = 20$), and L equal to twice the distance between points *b* and *c* (Fig. 5(b)).

Joining points *b* and *c* gives us straight line *cb*. The slope angle of straight line *cb* is α. Because principal lines curve so little, the direction of the next line segment should not vary much. Therefore we employ directional line detectors H_1^α, H_2^α to extract the line segments in this ROI and then keep all of the branches connecting with *ac* (Fig. 5(c)). If only one branch connected with *ac*, this branch is regarded as the next line segment. Otherwise, we choose one branch as follows. In Fig. 5(c), two branches, *cok* and *coh*, are connected with *ac* in ROI, where Point *o* is the branch point. Fig. 5(d) show the enlarged version of the ROI. We trace the line *oh*, *ok* and *oc* from point *o* and get the *N*th points *f*, *g* and *e*, respectively (here $N = 10$), and then link up *of*, *og* and *oe*, and compute Angle *foe* and Angle *goe*. The

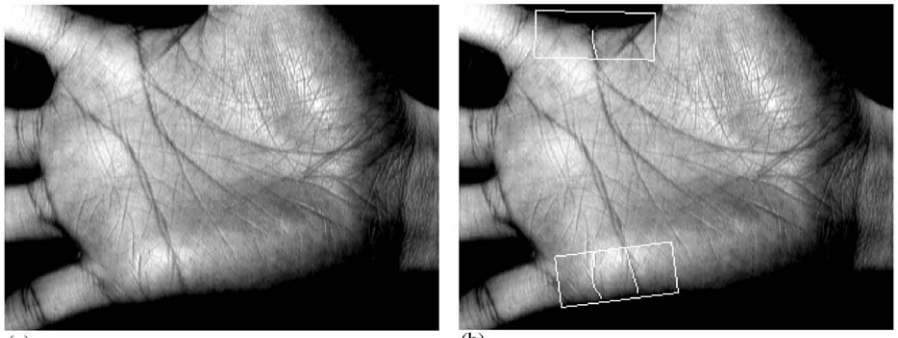

Fig. 4. Potential line initials of the principal lines: (a) original palmprint; (b) palmprint overlaid with the extracted potential line initials of the principal lines.

branch (oh) corresponding to the maximum angle is chosen as the next line segment.

After obtaining the next line segment, we should determine whether the heart line reaches its endpoint. We regard the heart line as having reached its endpoint if the line ch in the ROI satisfies one of the following two conditions:

(1) If the minimum distance from endpoint h *to* three sides of the ROI (not including the side passing through point c) exceeds a threshold T_d (here $T_d = 5$), point h is the endpoint.
(2) If Angle cmh is less than a threshold T_a (here T_a=135°), having joined points c and h, having supposed that point m is the farthest point to the straight line ch on curve ch, and having joined cm and hm, point m is the endpoint (Fig. 5(e)).

If the curve ch satisfies none of these conditions, we take the longer curve ah as the current extracted heart line and repeat this process recursively until the extracted curve reaches its endpoint.

Fig. 5(f) shows the whole extracted heart line and (g) is the palmprint overlaid with the whole heart line and all of the ROIs involved in this heart line extraction.

4.4. Extracting life and head lines

The process of extracting the life line and the head line differs little from that of extracting the heart line. The difference is in the rule that only one line may be extracted from each line initial. While this works well in heart line extraction, it is unsuitable for life line and head line extraction because life line and head line may share their line initials. Given this, we apply our observation that the branch point of the life line and head line should not exceed line-segment NK and LK (Fig. 1(b)). With this in mind, when using the recursive heart line extraction process to extract the life line and head line, if the extracted curve does not run across line-segment NK and LK and if there exists more than one branch, instead of choosing just one of the branches, we extract and trace the curves from each branch. If the extracted curve crosses line-segment NK or LK, the extraction process is the same as for heart line extraction.

Fig. 6 illustrates the process of life line and head line extraction. In this figure, (a) is the extracted line including two branches. In the original heart line extraction process, only one branch (oe) would be chosen and the other one (of) would be discarded. Obviously, it is wrong to discard branch of because it is a part of the life line. Since the extracted line does not run across line-segment NK and LK, we split this branched curve into two curves aoe and aof (Fig. 6(b) and (c)) and extract the lines from each of them. In this figure, the extracted curve related with aoe is the head line (Fig. 6(d)) and the one related with aof is the life line (Fig. 6(e)). Fig. 6(f) shows the palmprint overlaid with all of the extracted principal lines.

5. Palmprint classification

To classify a palmprint, we first extract its principal lines and then classify the palmprint by the number of the principal lines and the intersections of these principal lines. As the number of each type of principal line is less than or equal to 1, there are at most three principal lines. Two principal lines are said to intersect only if some of their points overlap or some points of one line are the neighbors of some points of another line. If any two principal lines intersect, the number of intersections increases by 1. Therefore, the number of intersections of three principal lines is less than or equal to 3.

Regarding the number of their principal lines and the number of the intersections of these lines, palmprints can be classified into following six categories (Table 1):

Category 1: Palmprints composed of no more than one principal line (Fig. 7(a));

Category 2: Palmprints composed of two principal lines and no intersection (Fig. 7(b));

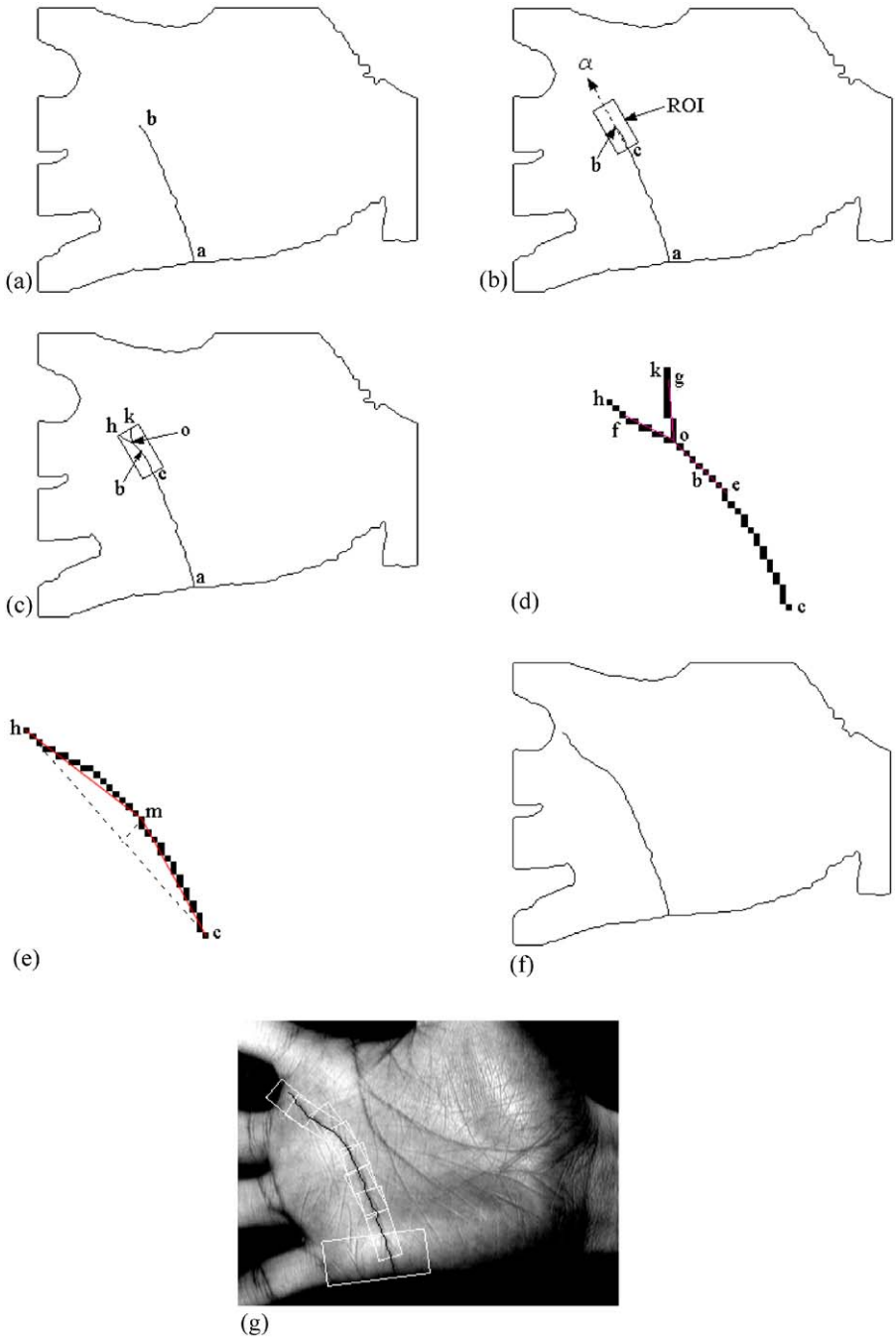

Fig. 5. Heart line extraction.

Category 3: Palmprints composed of two principal lines and one intersection (Fig. 7(c));

Category 4: Palmprints composed of three principal lines and no intersection (Fig. 7(d));

Category 5: Palmprints composed of three principal lines and one intersection (Fig. 7(e));

Category 6: Palmprints composed of three principal lines and more than one intersection (Fig. 7(f)).

The complete classification process for an input palmprint is as follows: (1) binary this palmprint and extract its boundary; (2) detect the key points; (3) extract heart line; (4) extract head line and life line; (5) calculate the number

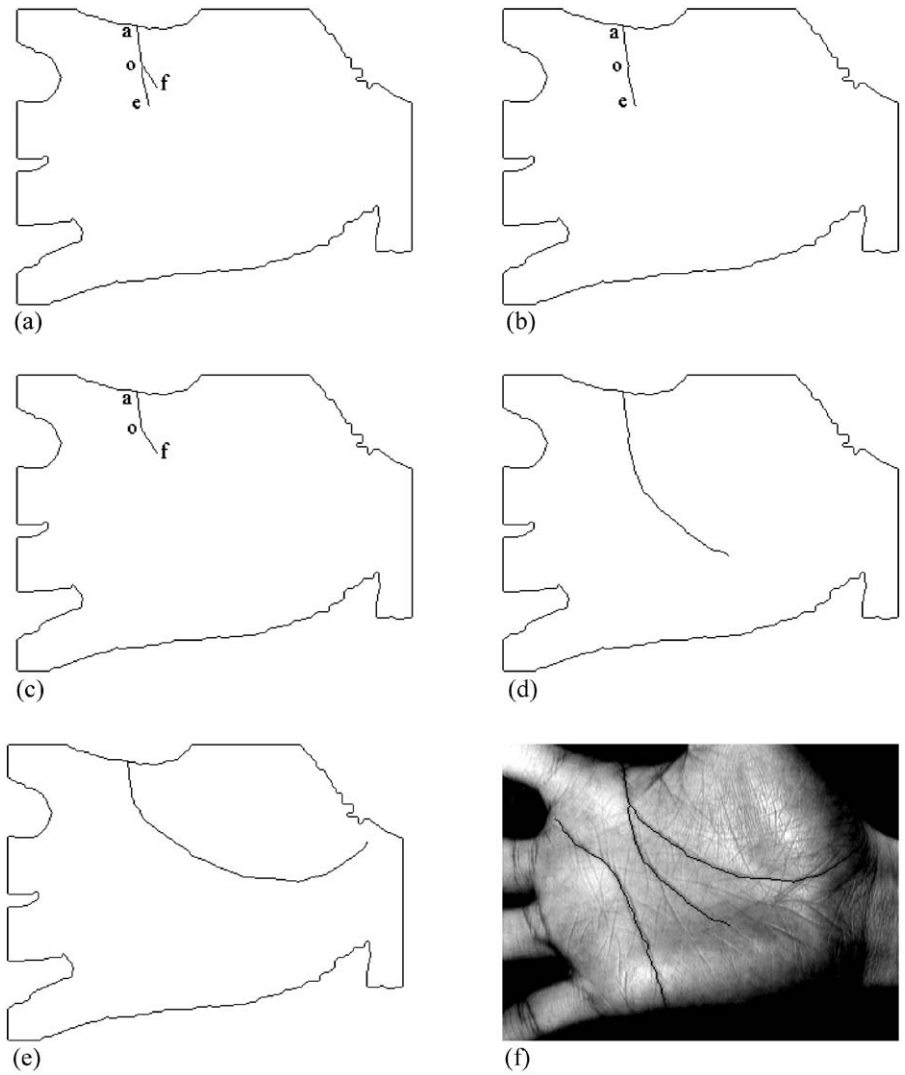

Fig. 6. Life line and head line extraction.

Table 1
Palmprint classification rules

Number of principal lines	$\leqslant 1$	2		3		
Number of the intersections of principal Lines	0	0	1	0	1	$\geqslant 2$
Category no.	1	2	3	4	5	6

of principal lines and their intersections; and (6) classify the palmprint into one of the defined categories using the classification rules.

6. Experimental results

Our palmprint classification algorithm was tested on a database containing 13,800 palmprints captured from 1,380 different palms using a CCD-camera-based device, 10 images per palm. The images are 320×240 with eight bits per pixel and the palmprints have been labeled manually. In this database, 0.36% samples belong to Category 1, 1.23% to Category 2, 2.83% to Category 3, 11.81% to Category 4, 78.12% to Category 5 and 5.65% to Category 6. The distribution of each category in our palmprint database is listed in Table 2.

Correct classification takes place when the palmprint is classified into a category whose label is same as the label of this palmprint. Misclassification takes place when the

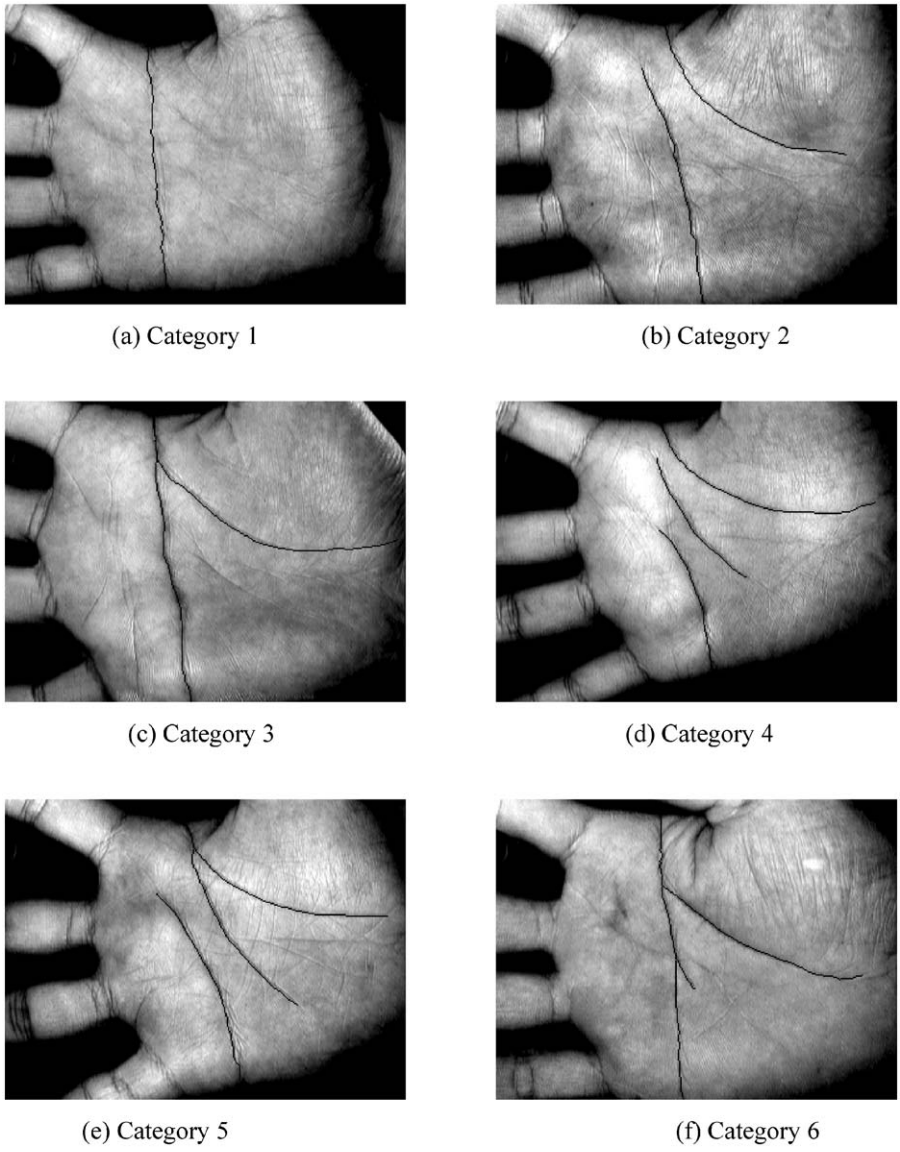

Fig. 7. Examples of each palmprint category.

Table 2
Distribution of each category in our database

Category no.	1	2	3	4	5	6
Number of palmprints	50	170	390	1,630	10,780	780
Percent (%)	0.36	1.23	2.83	11.81	78.12	5.65

palmprint is classified into a category whose label is different from the label of this palmprint. In all of the 13,800 palmprints in the database, 548 samples were misclassified: 7 in Category 1, 11 in Category 2, 25 in Category 3, 104 in Category 4, 349 in Category 5 and 47 in Category 6. The classification accuracy is about 96.03%. The confusion matrix is given in Table 3 and the classification accuracy in Table 4.

Table 3
Classification results of the proposed algorithm

Assigned category no.	True category no.					
	1	2	3	4	5	6
1	**43**	6	3	23	41	2
2	3	**159**	1	41	132	7
3	4	0	**365**	18	95	13
4	0	3	2	**1,526**	12	0
5	0	2	11	13	**10,431**	25
6	0	0	8	9	69	**733**

Table 4
Classification accuracy of the proposed algorithm

Total samples	Correctly classified samples	Misclassified samples	Classification accuracy
13,800	13,252	548	96.03%

7. Conclusions

As the first attempt to classify low-resolution palmprints, this paper presents a novel algorithm for palmprint classification using principal lines. Principal lines are defined and characterized by their position and thickness. A set of directional line detectors is devised for principal line extraction. By using these detectors, the potential line initials of the principal lines are extracted and then, based on the extracted potential line initials, the principal lines are extracted in their entirety using a recursive process. The local information about the extracted part of the principal line is used to decide a ROI and then a suitable line detector is chosen to extract the next part of the principal line in this ROI. After extracting the principal lines, we present some rules for palmprint classification. The palmprints are classified into six categories considering the number of the principal lines and their intersections. From the statistical results in our database containing 13,800 palmprints, the distributions of Categories 1–6 are 0.36%, 1.23%, 2.83%, 11.81%, 78.12% and 5.65%, respectively. The proposed algorithm classified these palmprints with 96.03% accuracy.

References

[1] D. Zhang, Automated Biometrics—Technologies and Systems, Kluwer Academic Publishers, Dordrecht, 2000.

[2] A. Jain, R. Bolle, S. Pankanti, Biometrics: Personal Identification in Networked Society, Kluwer Academic Publishers, Dordrecht, 1999.

[3] A. Jain, L. Hong, R. Bolle, On-line fingerprint verification, IEEE Trans. Pattern Anal. Mach. Intell. 19 (4) (1997) 302–313.

[4] L. Coetzee, E.C. Botha, Fingerprint recognition in low quality images, Pattern Recognition 26 (10) (1993) 1441–1460.

[5] R.P. Wildes, Iris recognition: an emerging biometric technology, Proc. IEEE 85 (9) (1997) 1348–1363.

[6] W.W. Boles, B. Boashash, A human identification technique using images of the iris and wavelet transform, IEEE Trans. Signal Process. 46 (4) (1998) 1185–1188.

[7] R. Brunelli, T. Poggio, Face recognition: features versus templates, IEEE Trans. Pattern Anal. Mach. Intell. 15 (10) (1993) 1042–1052.

[8] Y. Gao, M.K.H. Leun, Face recognition using line edge map, IEEE Trans. Pattern Anal. Mach. Intell. 24 (6) (2002) 764–779.

[9] J.P. Campbell Jr., Speaker recognition: a tutorial, Proc. IEEE 85 (9) (1997) 1437–1462.

[10] K. Chen, Towards better making a decision in speaker verification, Pattern Recognition 36 (2) (2003) 329–346.

[11] A.K. Jain, A. Ross, D. Prabhakar, An introduction to biometric recognition, IEEE Trans. on Circuits and Systems for Video Technology 14 (1) (2004) 4–20.

[12] N. Duta, A.K. Jain, K.V. Mardia, Matching of palmprint, Pattern Recogn. Lett. 23 (4) (2001) 477–485.

[13] D. Zhang, W. Kong, J. You, M. Wong, Online palmprint identification, IEEE Trans. Pattern Anal. Mach. Intell. 25 (9) (2003) 1041–1050.

[14] C.C. Han, H.L. Chen, C.L. Lin, K.C. Fan, Personal authentication using palm-print features, Pattern Recognition 36 (2) (2003) 371–381.

[15] A. Kumar, D.C.M. Wong I, H.C. Shen I, A. Jain, Personal verification using palmprint and hand geometry biometric, Lecture Notes in Computer Science, Vol. 2688, Springer, Berlin, 2003, pp. 668–678.

[16] K. Karu, A.K. Jain, Fingerprint classification, Pattern Recognition 29 (3) (1996) 389–404.

[17] R. Pelli, A. Lumini, D. Maio, D. Maltoni, Fingerprint classification by directional image partitioning, IEEE Trans. Pattern Anal. Mach. Intell. 21 (5) (1999) 402–421.

[18] W. Shu, G. Rong, Z. Bian, Automatic palmprint verification, Int. J. Image Graphics 1 (1) (2001) 135–151.

[19] R.M. Haralick, Ridges and valleys on digital images, Comput. Vision Graphics Image Process. 22 (1983) 28–38.

[20] K. Liang, T. Tjahjadi, Y. Yang, Roof edge detection using regularized cubic B-spline fitting, Pattern Recognition 30 (5) (1997) 719–728.

[21] J. Canny, A computational approach to edge detection, IEEE Trans. Pattern Anal. Mach. Intell. 8 (6) (1986) 679–698.

[22] J.R. Parker, Algorithms for Image Processing and Computer Vision, Wiley, New York, 1997.

About the Author—XIANGQIAN WU received his B.Sc. and M.Sc. degrees in Computer Science from Harbin Institute of Technology (HIT), China, in 1997 and 1999, respectively. He is currently a Ph.D. student in School of Computer Science and Technology at Harbin Institute of Technology (HIT). His research interests include pattern recognition, image analysis and biometrics, etc.

About the Author—DAVID ZHANG graduated in computer science from Peking University in 1974 and received his M.Sc. and Ph.D. degrees in computer science and engineering from Harbin Institute of Technology (HIT) in 1983 and 1985, respectively. From 1986 to 1988, he was a postdoctoral fellow at Tsinghua University and became an associate professor at Academia Sinica, Beijing, China. He received his second Ph.D. in electrical and computer engineering at University of Waterloo, Ontario, Canada, in 1994. Currently, he is a professor in Hong Kong Polytechnic University. He is the Founder and Editor-in-Chief, International Journal of Image and Graphics (IJIG); Book Editor, Kluwer International Series on Biometrics (KISB); and Program Chair, International Conference on Biometrics Authentication (ICBA). He is Associate Editor of more than ten international journals including IEEE Trans on SMC-A/SMC-C, Pattern Recognition, and is the author of more than 120 journal papers, twenty book chapters and nine books. As a principal investigator, He has since 1980 brought to fruition many biometrics projects and won numerous prizes. He holds a number of patents in both the USA and China and is a current Croucher Senior Research Fellow.

About the Author—KUANQUAN WANG received his BE and ME degrees from Harbin Institute of Technology (HIT), Harbin, China, and his Ph.D. degree in computer science and technology from Chongqing University, Chongqing, China, in 1985, 1988, and 2001, respectively. From 2000 to 2001 he was a visiting scholar in Hong Kong Polytechnic University supported by Hong Kong Croucher Funding. From 2003 to 2004 he was a research fellow in the same university. Currently, he is a professor and a supervisor of Ph.D. candidates of department of computer science and engineering, and an associate director of Biocomputing Research Centre in HIT. So far, he has published over 70 papers. Also he is a member of the IEEE, an editorial board member of International Journal of Image and Graphics. His research interests include biometrics, image processing and pattern recognition.